

Interactions and oscillations in quantum dots

This article has been downloaded from IOPscience. Please scroll down to see the full text article.

1999 J. Phys.: Condens. Matter 11 229

(<http://iopscience.iop.org/0953-8984/11/1/019>)

View [the table of contents for this issue](#), or go to the [journal homepage](#) for more

Download details:

IP Address: 171.66.16.210

The article was downloaded on 14/05/2010 at 18:21

Please note that [terms and conditions apply](#).

Interactions and oscillations in quantum dots

Jia-Lin Zhu^{†‡}, Ziqiang Zhu[§], Yoshiyuki Kawazoe[§] and Takafumi Yao[§]

[†] Department of Physics, Tsinghua University, Beijing 100084, People's Republic of China

[‡] Centre for Interdisciplinary Research, Tohoku University, Sendai 980-8578, Japan

[§] Institute for Materials Research, Tohoku University, Sendai 980-8577, Japan

Received 19 June 1998, in final form 29 September 1998

Abstract. The exact ion–electron and electron–electron interaction energies in quantum dots (QDs) with parabolic potentials are calculated and studied in detail. On the basis of calculated results, one- and two-electron spectra in QDs are revealed. It is found that the spectra are dramatically changed with the variation of the size and field. The even-parity–odd-parity and spin-singlet–spin-triplet oscillations with magnetic field are clearly shown for one- and two-electron ground states in QDs. The variations of the spectra with field are quite different for different dot sizes, and represent magnetic ‘fingerprints’ of the QDs. These phenomena are induced by the negative-ion–electron and electron–electron interactions in QDs.

1. Introduction

Recently, advances in nanofabrication technology have made it possible to manufacture quantum dots (QDs) containing one, two, and more electrons, which have been intensively investigated experimentally and theoretically. The study of semiconductor QDs is expanding rapidly [1–6], and ion–electron and electron–electron interactions are shown to be of great importance [7–12] in such systems. Departures from the single-particle picture due to electron–electron interaction in QDs have been observed [9–12]. Applying a magnetic field to QDs with a few electrons can reveal various spectra—so-called magnetic ‘fingerprints’—since the spectra of QDs are governed by the interplay of two energy scales: the Coulomb interactions and the confinement energy associated with quantization due to the confining potential. It has been experimentally found that a magnetic field can induce transitions between the ground and excited states in semiconductor QDs containing a few electrons [11].

The semiconductor QDs are ideal quasi-zero-dimensional structures to study, since the effective-mass theory can be used for an appropriate regime of quantum size. As is well known, studying the electronic structures in quantum wells (QWs) with and without strong magnetic fields is an important problem in semiconductor physics. QWs with strong magnetic fields can, in fact, form some kinds of QD, while a strong magnetic field can change the confining potential of the QDs and then the corresponding spectra including the Zeeman term. Therefore, studies of electronic structures in QDs containing a few electrons with and without magnetic fields are of interest both in their own right and in assisting one to understand the role of strong magnetic fields in QWs and QDs.

It is very important to have reliable methods for solving the many-electron problem and showing the characteristics of electronic structures in QDs. The main approaches to the problem include ‘exact’ numerical diagonalization [7, 8], numerical simulations based on

quantum Monte Carlo techniques [13], and Hartree–Fock calculations [7, 14–16]. For two electrons in circular QDs with parabolic potentials, exact solutions have been obtained [17].

In the last few years there has been increasing interest in the study of two electrons in quantum dots in a magnetic field [17–20]. It produces energy spectra and related properties due to the electron–electron interaction and the Pauli exclusion. On the basis of a first-order perturbation calculation of the Coulomb energy, the spin oscillations with the magnetic field are also shown [20]. In order to show the quantum-size effect, the spin oscillation, and its magnetic fingerprint correctly, a reliable method is needed. To our knowledge, there have been no reports related to the exact solutions for two electrons in QDs in a magnetic field that might reveal the field effects on the spectra, including highly excited states.

For the single-electron spectra of QWs with a magnetic field, the effects of the field and positively charged ion have been shown and studied in detail [21]. In order to exactly show the field and ion effects on the single- and two-electron spectra of QDs and to understand better the characteristics of ion–electron and electron–electron interactions in confined systems, negative-ion–electron and electron–electron interaction energies in QDs are calculated by using the series expansion method [17, 21] in this paper. Interesting phenomena, such as parity or spin oscillations and their magnetic fingerprints mentioned above, are clearly shown by the calculated results.

The rest of this paper is organized as follows. The Hamiltonian and the calculation method are presented in section 2. The main results are given and discussed in section 3. This is followed by a summary, in section 4.

2. The model

For some real dots, a harmonic oscillator is a very good approximation for describing the lateral confinement of the electrons [1, 14], where the motion in the z -direction is always frozen out into the lowest subband [22]. The finite width of the dot layer can alter the electron–electron interaction but cannot change the order of the interaction energies in QDs [17, 22]. To study the oscillation and its magnetic fingerprint, the dots can be treated as two-dimensional limits of thin discs. Hence, it is reasonable to write the Hamiltonian of an electron in such a parabolic quantum dot with a negatively charged impurity (ion) centre—for example, an occupied acceptor centre—as follows:

$$H_{i0} = -\nabla^2 + \frac{1}{4}\gamma_d^2\rho^2 + \frac{2}{\rho}. \quad (1)$$

It is also reasonable to write the Hamiltonian of two electrons in such a parabolic quantum dot in the form

$$H_0 = -\nabla_1^2 - \nabla_2^2 + \frac{1}{4}\gamma_d^2\rho_1^2 + \frac{1}{4}\gamma_d^2\rho_2^2 + \frac{2}{|\vec{\rho}_1 - \vec{\rho}_2|} \quad (2)$$

where effective atomic units are used. The effective Rydberg R^* and the effective Bohr radius a^* are taken to be the energy and length units, respectively. It is easy to see that $\gamma_d^{-1/2}$ is related to the confinement region of the electrons in the dot.

Applying a magnetic field \vec{B} perpendicular to the x – y plane, equations (1) and (2) are respectively turned into

$$H_i = H_{i0} + \frac{1}{4}\gamma^2\rho^2 + \gamma L_z \quad (3)$$

and

$$H = H_0 + \frac{1}{4}\gamma^2\rho_1^2 + \frac{1}{4}\gamma^2\rho_2^2 + \gamma L_{z1} + \gamma L_{z2} \quad (4)$$

where the magnetic field is measured in units of $\hbar\omega_c/2R^*$ with ω_c the cyclotron frequency. γL_{z1} and γL_{z2} are the Zeeman terms induced by the magnetic field. It is interesting to see how large the units of semiconductor materials are. For GaAs materials, for example, $R^* = 5.8$ meV, $a^* = 10$ nm, and $\gamma = 1$ corresponds to $B = 6.75$ T.

The Hamiltonian of equation (4) can be separated into centre-of-mass and relative-motion terms as follows:

$$H = H_R + H_r \quad (5)$$

with

$$H_R = -\frac{\nabla_R^2}{2} + \frac{1}{2}\Gamma^2 R^2 + \gamma L_{ZR} \quad (6)$$

and

$$H_r = -2\nabla_r^2 + \frac{1}{8}\Gamma^2 r^2 + \gamma L_{zr} + \frac{2}{r} \quad (7)$$

where $\Gamma^2 = \gamma^2 + \gamma_d^2$, $\vec{R} = (\vec{\rho}_1 + \vec{\rho}_2)/2$, $\nabla_R = \nabla_1 + \nabla_2$, $\vec{r} = \vec{\rho}_1 - \vec{\rho}_2$, and $\nabla_r = (\nabla_1 - \nabla_2)/2$. L_{ZR} and L_{zr} are the Z- and z-component angular momentum operators in the centre-of-mass and relative-motion systems, respectively. This separability and the cylindrical symmetry of the problem allow us to write the two-particle wave functions in plane polar coordinates $\vec{r} = (r, \varphi)$ in the form $\Phi(R)\phi(r)\exp(im\varphi)$. The spatial part of the total wave function is symmetric (antisymmetric) with respect to particle permutation ($\varphi \rightarrow \varphi + \pi$) for even (odd) azimuthal quantum numbers m . Since the Pauli exclusion principle requires the total wave function to be antisymmetric, we have spin-singlet ($s = 0$) and spin-triplet ($s = 1$) states for even and odd m , respectively. The energy eigenvalues of equation (6) are given by

$$E(N, M) = (2N + |M| + 1)\Gamma + M\gamma \quad (8)$$

in terms of the radial ($N = 0, 1, 2, \dots$) and azimuthal ($M = 0, \pm 1, \pm 2, \dots$) quantum numbers. The eigenvalues of the relative motion excluding the electron–electron interaction are also in the same kind of form, and are given by

$$E_0(n, m) = (2n + |m| + 1)\Gamma + m\gamma \quad (9)$$

in terms of the corresponding radial and azimuthal quantum numbers $n = 0, 1, 2, \dots$ and $m = 0, \pm 1, \pm 2, \dots$. However, we should solve the Schrödinger-like equation

$$H_r[\phi(r)\exp(im\varphi)] = E(m)[\phi(r)\exp(im\varphi)] \quad (10)$$

to get the energy of the relative motion including the electron–electron interaction. It is easy to find the equation satisfied by the function $\phi(r)$:

$$\frac{d^2\phi}{dr^2} + \frac{1}{r}\frac{d\phi}{dr} + \left(\frac{E(m) - m\gamma}{2} - \frac{1}{r} - \frac{m^2}{r^2} - \frac{1}{16}\Gamma^2 r^2\right)\phi = 0. \quad (11)$$

We can use the method of series expansion [17, 21] to obtain exact series forms in different regions from equation (11). In the region $0 < r$, we have a series solution, which has a finite value at $r = 0$, as follows:

$$\phi(r) = Ar^{|m|} \sum_{n=0}^{\infty} a_n r^n \quad (12)$$

where A is a constant and a_0 is equal to 1. Noting that the a_n are equal to zero when n is equal to a negative integer, the other a_n can be determined by the following recurrence relation:

$$a_n = (2a_{n-1} + (m\gamma - E(m))a_{n-2} + \frac{1}{8}\Gamma^2 a_{n-4}) / (4|m| + 2n)n \quad \text{for } n = 1, 2, 3, \dots \quad (13)$$

In the region $r < \infty$, we can obtain a normal solution in the form

$$\phi(r) = B \exp\left(-\frac{1}{8}\Gamma r^2\right) r^s \sum_{n=0}^N b_n r^{-n} \quad (14)$$

where

$$s = (E(m) - m\gamma) / \Gamma - 1 \quad (15)$$

$$b_0 = b_1 = 1 \quad (16)$$

$$b_n = 2b_{n-1} - [(s - n + 2)^2 - m^2]b_{n-2} \quad \text{for } n = 2, 3, 4, \dots$$

and B is a constant. At R_1, R_2, \dots and R_T , exact forms of uniformly convergent Taylor series can be found. Using the matching conditions at $r = R_i$ ($i = 1, 2, \dots, T$) and the 2×2 transfer matrices, we deduce the equation for the eigenenergies $E(n, m)$ easily. The values of $E(n, m)$ and $\phi_{nm}(r)$ are obtained numerically.

For the sake of convenience, we define the electron–electron interaction energies $E_r(n, m)$ as the difference between $E(n, m)$ and $E_0(n, m)$, i.e.,

$$E_r(n, m) = E(n, m) - E_0(n, m). \quad (17)$$

Then, the energy eigenvalues of the Hamiltonian given as equation (4) are the sums of $E(n, m)$ and $E(N, M)$ as follows:

$$E(n, m; N, M) = [2(N + n) + |M| + |m| + 2]\Gamma + [M + m]\gamma + E_r(n, m). \quad (18)$$

The case is similar for H_i of equation (3). The eigenvalues $E_{i0}(n_i, m_i)$ of H_i excluding the ion–electron interaction are given by

$$E_{i0}(n, m) = (2n_i + |m_i| + 1)\Gamma + m_i\gamma \quad (19)$$

in terms of the corresponding radial and azimuthal quantum numbers $n_i = 0, 1, 2, \dots$ and $m_i = 0, \pm 1, \pm 2, \dots$. Using the same procedure as mentioned above, we can easily obtain the eigenenergies $E_i(n_i, m_i)$ of H_i . Then, we can define the ion–electron interaction energies $E_{ie}(n_i, m_i)$ as the differences between $E_i(n_i, m_i)$ and $E_{i0}(n_i, m_i)$, i.e.,

$$E_{ie}(n_i, m_i) = E_i(n_i, m_i) - E_{i0}(n_i, m_i). \quad (20)$$

The energy levels of H_i in equation (3) are as follows:

$$E_i(n_i, m_i) = (2n_i + |m_i| + 1)\Gamma + m_i\gamma + E_{ie}(n_i, m_i). \quad (21)$$

3. Results and discussion

The levels $E(n, m; N, M)$ can be labelled by four symbols, n, m, N , and M . The even and odd m correspond to the spin-singlet ($s = 0$) and spin-triplet ($s = 1$) states, respectively, because of the Pauli exclusion principle. The notation 1s, 2p, 2s, 3d, 3p (1S, 2P, 2S, 3D, 3P), and so on, is used if the principal quantum numbers $n_p = n + |m| + 1$ ($N_p = N + |M| + 1$) are used instead of n (N), and s, p, d, ... (S, P, D, ...) for $|m|$ ($|M|$) = 0, 1, 2, ... This is simple for the single-electron levels. The $E_i(n_i, m_i)$ are indicated by the two symbols n_i and m_i . We can also have 1s, 2s, 2p, 3d, and so on, as mentioned above.

3.1. $E_{ie}(n_i, m_i)$ and $E_r(n, m)$

To achieve a better understanding of quantum-size and ion effects, and parity and spin oscillations and the magnetic fingerprint, which will be discussed in the rest of this section, it is interesting to study the ion–electron and electron–electron interaction energies, $E_{ie}(n_i, m_i)$

Table 1. Electron–electron interaction energies $E_r(n, m)$ of two electrons in QDs with different Γ . The values in brackets were obtained by using equation (23).

Γ	0.05	0.1	0.2	0.4	1.0	2.5	4.0	5.0
$E_r(0, 0)(1s)$	0.1963 (0.3963)	0.3081 (0.5605)	0.4816 (0.7927)	0.7494 (1.1210)	1.3195 (1.7725)	2.2803 (2.8025)	2.9930 (3.5449)	3.3988 (3.9633)
$E_r(1, 0)(2s)$	0.1853	0.2871	0.4413	0.6723	1.1473	1.9154	2.4721	2.7862
$E_r(2, 0)(3s)$	0.1763	0.2703	0.4106	0.6000	1.0333	1.6967	2.1744	2.4435
$E_r(0, 1)(2p)$	0.1562 (0.1982)	0.2333 (0.2802)	0.3451 (0.3963)	0.5066 (0.5605)	0.8279 (0.8862)	1.3404 (1.4012)	1.7107 (1.7725)	1.9195 (1.9817)
$E_r(1, 1)(3p)$	0.1468	0.2168	0.3170	0.4637	0.7438	1.1941	1.5188	1.7017
$E_r(0, 2)(3d)$	0.1311 (0.1486)	0.1915 (0.2102)	0.2776 (0.2972)	0.3998 (0.4204)	0.6436 (0.6647)	1.0294 (1.0509)	1.3078 (1.3293)	1.4645 (1.4862)
$E_r(1, 2)(4d)$	0.1240	0.1799	0.2594	0.3784	0.5957	0.9496	1.2047	1.3485

and $E_r(n, m)$, defined by equations (17) and (20) at first. It is also interesting to note that for a fixed state, both depend only on Γ , and that the values of $E_{ie}(n_i, m_i)$ can be obtained from those of $E_r(n, m)$ by changing the scale. Therefore, only the $E_r(n, m)$ are shown in table 1. It is readily seen that the $E_r(n, m)$ increase with Γ , and the ordering is as follows:

$$E_r(0, 0) > E_r(1, 0) > E_r(2, 0) > E_r(0, 1) > E_r(1, 1) > E_r(0, 2) > E_r(1, 2) \dots$$

We should point out that the ordering will be changed if the form of the confining potential of the QDs is changed. It is, however, important to note that, for a fixed n , the $E_r(n, m)$ always decrease with increasing $|m|$ because of the departure of the wave functions from the Coulomb centre.

It is accurate enough to calculate the $E_r(n, m)$ using first-order perturbation, as Γ is sufficiently large compared with the electron–electron interaction. Then, the $E_r(n, m)$ are given by

$$E_r(n, m) = \langle \phi_{nm}(r) | \frac{2}{r} | \phi_{nm}(r) \rangle \quad (22)$$

where the $\phi_{nm}(r)$ are normalized radial wave functions of equation (11) without the electron–electron interaction term. Using equation (22), we can easily find the ordering mentioned above. Furthermore, the values are proportional to $\Gamma^{1/2}$ and always larger than the corresponding ones obtained from the exact solutions. For $n = 0$, for example, the values given by equation (22) are as follows:

$$E_r(0, m) = \begin{cases} (\pi\Gamma)^{1/2} & \text{if } m = 0 \\ (\pi\Gamma)^{1/2} \frac{(2|m| - 1)!!}{2|m|!!} & \text{if } |m| > 0. \end{cases} \quad (23)$$

On comparing with the exact values shown in table 1, it is obvious that the larger the Γ and $|m|$ are, the less the difference between them is. It is reasonable to fit the exact values into the $\Gamma^{1/2}$ relation if Γ is large enough.

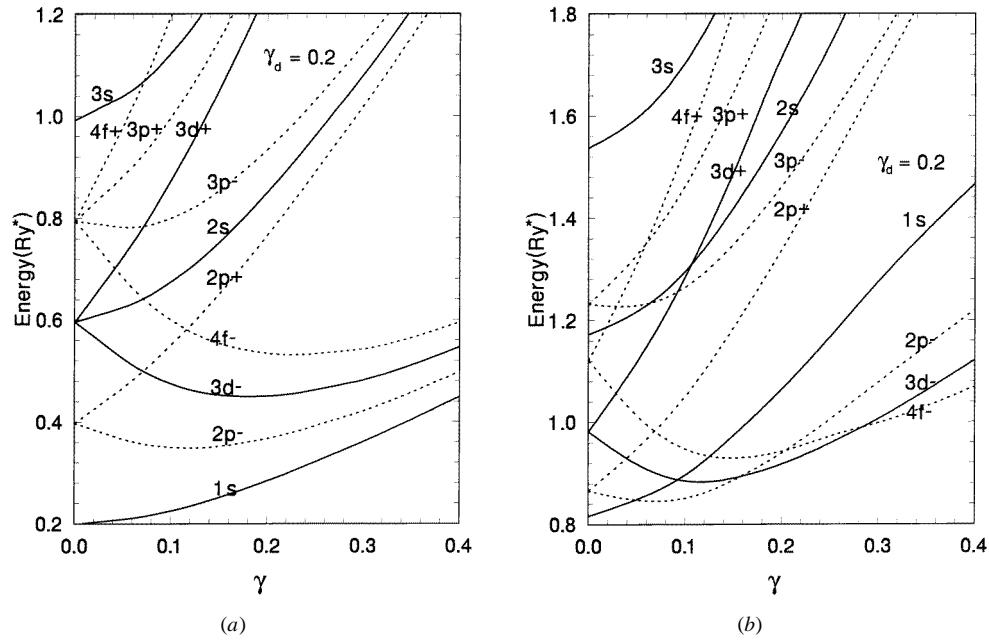


Figure 1. $E_i(n_i, m_i)$ versus γ for $1s, 2p_{\pm}, 3d_{\pm}, 4f_{\pm}, 2s, 3p_{\pm},$ and $3s$ states in the quantum dot with $\gamma_d = 0.2$ excluding the ion–electron interaction (a), and including the interaction (b). The solid and dotted curves represent even-parity and odd-parity states, respectively.

3.2. Ion effects and parity oscillations

In order to better understand the role of a negatively charged impurity (ion) in the single-electron spectra of QDs in a magnetic field, in figures 1(a) and 1(b) we have plotted the energy levels of an electron as a function of γ for QDs with $\gamma_d = 0.2$ without and with the ion centre, respectively. The splitting of the energy levels as γ increases from zero can be easily seen from figure 1(a). For example, the p states are each split into two levels with $m = -1$ and 1 . With increasing γ , the lower levels first decrease and then increase, while the higher levels increase monotonically. However, there is no splitting for s states. All of the energy levels approach the Landau levels or the corresponding s levels as γ approaches infinity. Clearly there are minima for the states with negative integer values of m . This is because of the two interactions of the Zeeman term and the parabolic potential in a range of small γ . The other feature of the figure is the interactions between different states before the strong-field limits are approached.

The ion–electron interaction can significantly change the spectra in QDs in a magnetic field if γ is of the same order of magnitude as γ_d . As shown in figure 1(b), the degeneracy is partly lifted by the interaction when $\gamma = 0$, and it is completely lifted when $\gamma > 0$. The level ordering and the interactions between different states are quite different from those shown in figure 1(a). An obvious feature of figure 1(b) induced by the interaction is the intersections of the lower levels. It leads to the parity oscillations of the ground states with γ , i.e., $1s-2p_- -3d_- -4f_-$, and so on. Moreover, on using $\gamma_d = 1$ instead of $\gamma_d = 0.2$ in the calculations above, we found that the oscillations still appear, but with different values of γ .

On the basis of the discussion in section 3.1, we explain the oscillations as follows. For $n_i = 0$, the level increases with increasing $|m_i|$ when $\gamma = 0$. On the other hand, the levels

with $n_i = 0$, excluding the interaction, approach the first Landau level as $\gamma \rightarrow \infty$. For a fixed γ with $n_i = 0$, however, the ion–electron interaction energies decrease with increasing $|m_i|$. This is why the even–parity–odd–parity oscillations with magnetic field appear.

3.3. Quantum-size effects

The two-electron spectra are slightly more complicated and are different from the single-electron ones. It is better to look at the quantum-size effects on the spectra before studying the magnetic fingerprint.

Table 2. Exact quantum levels of two electrons in QDs with different γ_d ($\gamma_d^{-1/2}$). The level sequences are in order of increasing magnitude. For the sake of convenience, shortened notation, i.e., a, b, c, and so on, is used to indicate the quantum numbers ($n, m; N, M; s$) and to show the changes of the level order. The energy unit is R^* .

γ_d ($\gamma_d^{-1/2}$)	1.0 (1.0)	0.2 (2.2361)	0.05 (4.4721)
a: (0, 0; 0, 0; 0)	(a) 3.3196	(a) 0.8816	(a) 0.2962
b: (0, 1; 0, 0; 1)	(b) 3.8278	(b) 0.9450	(b) 0.3062
c: (0, 0; 0, 1; 0)	(c) 4.3196	(d) 1.0776	(d) 0.3310
d: (0, 2; 0, 0; 0)	(d) 4.6436	(c) 1.0816	(c) 0.3462
e: (0, 1; 0, 1; 1)	(e) 4.8278	(e) 1.1450	(h) 0.3476
f: (1, 0; 0, 0; 0)	(f) 5.1472	(h) 1.2156	(e) 0.3562
g: (0, 0; 1, 0; 0)	(g) 5.3196	(f) 1.2402	(i) 0.3810
h: (0, 3; 0, 0; 1)	(h) 5.5174	(i) 1.2776	(f) 0.3854
i: (0, 2; 0, 1; 0)	(i) 5.6436	(g) 1.2816	(g) 0.3962
j: (1, 1; 0, 0; 1)	(j) 5.7438	(j) 1.3170	(j) 0.3968
k: (0, 1; 1, 0; 1)	(k) 5.8278	(k) 1.3450	(k) 0.4062
l: (1, 0; 0, 1; 0)	(l) 6.1472	(n) 1.4053	(n) 0.4066
m: (0, 0; 1, 1; 0)	(m) 6.3196	(l) 1.4402	(o) 0.4240
n: (0, 4; 0, 0; 0)	(n) 6.4693	(o) 1.4594	(p) 0.4310
o: (1, 2; 0, 0; 0)	(o) 6.5956	(p) 1.4776	(l) 0.4354
p: (0, 2; 1, 0; 0)	(p) 6.6436	(m) 1.4816	(m) 0.4462

As shown in table 2, the two-electron spectra vary not only in their values but also in their level ordering as γ_d ($\gamma_d^{-1/2}$) changes from 0.05 (4.4721) to 1 (1). An important aspect of the quantum-size effects is the changes of the level ordering and the level differences; a crossover of two levels with the same or different spin can appear when γ_d ($\gamma_d^{-1/2}$) is less (greater) than one. The reason for this is the following. The values of $E_r(n, m)$ are approximately proportional to $\gamma_d^{1/2}$ for $\gamma = 0$ as mentioned in section 3.1. However, both $E(N, M)$ and $E_0(n, m)$ are proportional to γ_d . When γ_d ($\gamma_d^{-1/2}$) is greater (less) than one, the level ordering is mainly determined by the sum of $E_0(n, m)$ and $E(N, M)$. It can be strongly changed by $E_r(n, m)$ if γ_d ($\gamma_d^{-1/2}$) is much less (greater) than one. Therefore the quantum-size effects appear.

3.4. Singlet–triplet oscillation and the magnetic fingerprint

In order to better understand the role of the electron–electron interaction in two-electron spectra of QDs in a magnetic field, in figures 2(a) and 2(b) we have plotted the energy levels as functions of γ for QDs with $\gamma_d = 0.2$ without and with the interaction, respectively. As shown in the figures, the splitting of the energy levels is induced by the Zeeman terms as γ increases from zero. For the sake of clarity, we have only plotted the lower levels in the figures. With

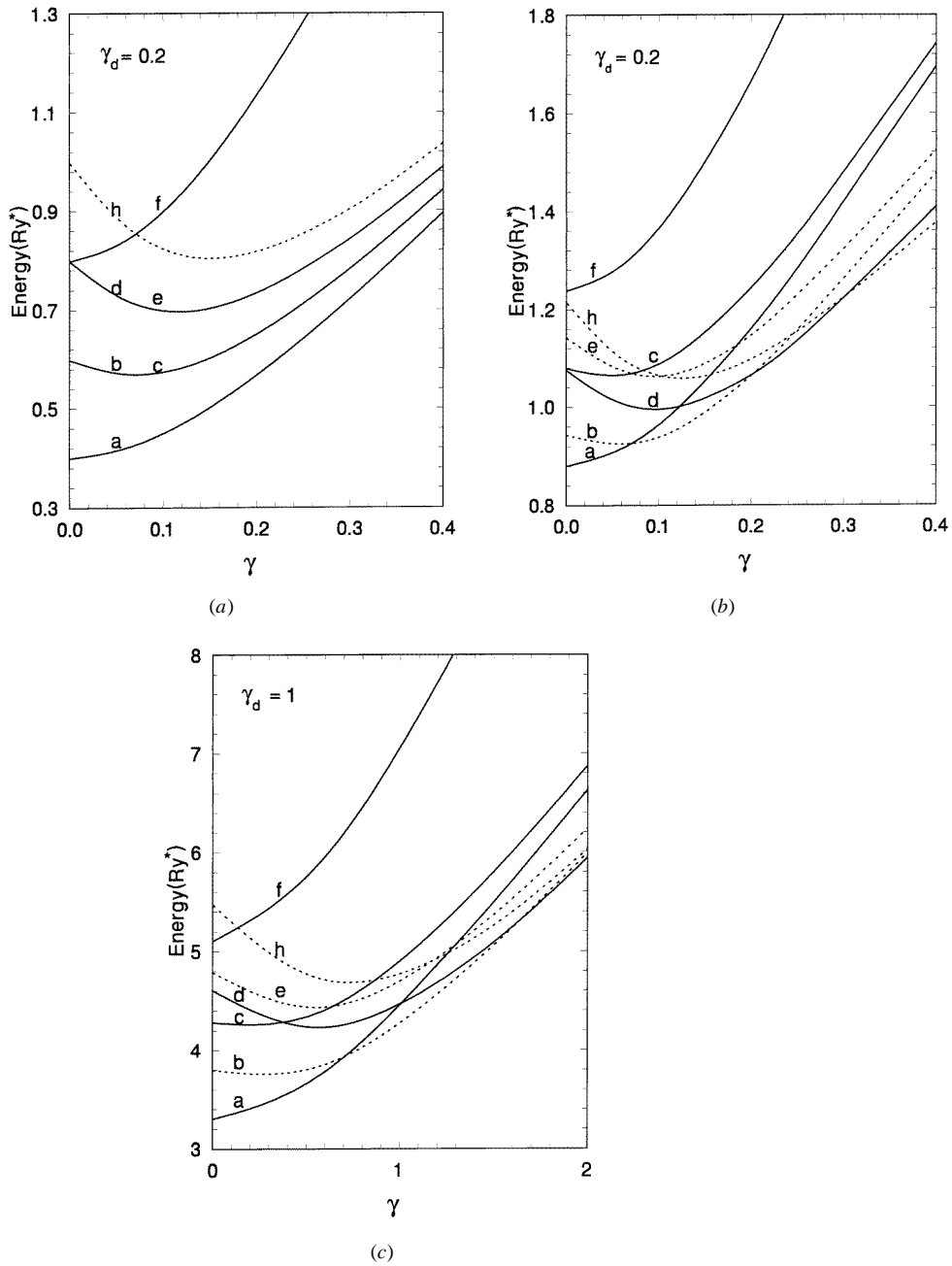


Figure 2. $E(n, m; N, M)$ versus γ for the a, b, c, d, e, f, and h states indicated in table 2 for the quantum dot with $\gamma_d = 0.2$ excluding the electron–electron interaction (a), that including the interaction (b), and the dot with $\gamma_d = 1$ including the interaction (c). For the sake of clarity, only the lower levels are plotted. The solid and dotted curves represent spin-singlet and spin-triplet states, respectively.

increasing γ , the lower levels first decrease and then increase. There are minima for the states with negative integer values of m . This is due to the two interactions of the Zeeman term and the parabolic potential in a range of small γ . However, there is no splitting for the states with $M = m = 0$, and the levels increase monotonically.

The electron–electron interaction can significantly change the spectra of QDs in a magnetic field. As shown in figure 2(b), the degeneracy is lifted by the interaction when $\gamma = 0$. The level ordering is changed with increasing γ , and interactions between different states appear. An obvious feature of figure 2(b) induced by the interaction is the interactions between the lower levels. They lead to the spin-singlet–spin-triplet oscillations of the ground states with γ i.e., a–b–d–h states, and so on, shown in the figure.

On the basis of the discussion in section 3.1, we explain the oscillations as follows. For $N = n = 0$, the level increases with increasing $|m|$ when $\gamma = 0$. On the other hand, the levels with $N = n = 0$ and negative integer values of m , excluding the interaction, approach the same level as $\gamma \rightarrow \infty$. For fixed γ , however, the interaction energies decrease with increasing $|m|$. This means that the level sequence of a–b–d–h states, and so on, is in order of decreasing magnitude as $\gamma \rightarrow \infty$. This is why the spin-singlet–spin-triplet oscillations with magnetic field appear.

It is interesting to compare the above spectra with the others for QDs of different sizes to see what kind of difference appears and the importance of the role of electron–electron interaction in various spectra. For this purpose, we have calculated the spectra using $\gamma_d = 1$ instead of $\gamma_d = 0.2$. First, we should point out that the spectra excluding the interaction are exactly the same as those shown in figure 2(a), except the different scales. So we do not plot them here. However, the two cases become quite different as soon as the interaction is included. When $\gamma = 0$, the level ordering is different because of the quantum-size effects mentioned above. The level ordering and the interactions are also different when $\gamma \neq 0$ as shown in figure 2(c). The oscillations appear in different regions of γ . What we have shown in figures 2(b) and 2(c) indicates that the electron–electron interaction could play an important part in the spectra and also is one of the effects that go to make up the magnetic fingerprints of QDs. The other effects may be induced by dot shapes, doping impurities, and so on. This would be worth working on.

4. Summary

We have used different series solutions for different regions of the radial equation of the relative motion of two electrons in QDs with parabolic potentials and of that of an electron in the QDs with an ion centre to obtain the exact solutions. The ion–electron and electron–electron interaction energies $E_{ei}(n_i, m_i)$ and $E_r(n, m)$ are calculated and shown to be dependent on n_i and m_i , and n and m , respectively. Both increase with increasing confinement (Γ), and the strong-confinement limits are proportional to $\Gamma^{1/2}$. In general, for a fixed n (n_i), the interaction energies decrease with increasing $|m|$ ($|m_i|$). The one- and two-electron spectra of the QDs are revealed, and the parity and spin oscillations and the magnetic fingerprints of the QDs are clearly shown. The phenomena are induced by the negative-ion–electron and electron–electron interactions in QDs.

The present results will be useful for achieving an understanding of the optical and magnetic properties of quantum-dot materials and for explaining the experimental phenomena related to ion–electron and electron–electron interactions in QDs. We should point out that the shape and size of the confinement potential including ions can be used to change the number of possible spin oscillations, and it is even possible to make them disappear [23, 24]. Finally, it can be expected that the appropriate electronic structures of QDs, and also related properties

such as the magnetic fingerprint, will be obtained if the sizes and shapes of the QDs with doping and also the numbers of electrons are better controlled. It is, therefore, very important to study the electronic structures of a few electrons with a few ions in QDs with different sizes and shapes.

Acknowledgments

The authors would like to thank the Information Science Group of the Institute for Materials Research, Tohoku University, for their continuous support of the HITAC S-3800/380 supercomputing system. One of the authors, J-L Zhu, expresses his sincere thanks to all of the members of the research group for their kind hospitality during his stay in Sendai.

References

- [1] Sikorski C and Merkt U 1989 *Phys. Rev. Lett.* **62** 2164
- [2] Demel T, Heitmann D, Grambow P and Ploog K 1990 *Phys. Rev. Lett.* **64** 788
- [3] Lorke A, Kotthaus J P and Ploog K 1990 *Phys. Rev. Lett.* **64** 2559
- [4] Ashoori R C, Stormer H L, Weiner J S, Pfeiffer L N, Baldwin K W and West K W 1993 *Phys. Rev. Lett.* **71** 613
- [5] Alsmeyer J, Batke E and Kotthaus J P 1990 *Phys. Rev. B* **41** 1699
- [6] Meurer B, Heitmann D and Ploog K 1992 *Phys. Rev. Lett.* **68** 1371
- [7] Pfannkuche D, Gudmundsson V and Maksym P 1993 *Phys. Rev. B* **47** 2244
- [8] Maksym P A and Chakraborty T 1990 *Phys. Rev. Lett.* **65** 108
- [9] Matulis A and Peeters F M 1994 *J. Phys.: Condens. Matter* **6** 7751
- [10] Tarucha S, Austing D G, Honda T, van der Hage R J and Kouwenhoven L P 1996 *Phys. Rev. Lett.* **77** 3613
- [11] Kouwenhoven L P, Oosterkamp T H, Danoesastro M W S, Eto M, Austing D G, Honda T and Tarucha S 1997 *Science* **278** 1788
- [12] Stewart D R, Sprinzak D, Marcus C M, Duruoz C I and Harris J S Jr 1997 *Science* **278** 1784
- [13] Bolton F 1994 *Solid-State Electron.* **37** 1159
- [14] Kumar A, Laux S E and Stern F 1990 *Phys. Rev. B* **42** 5166
- [15] Broido D A, Kempa K and Bakshi P 1990 *Phys. Rev. B* **42** 11 400
- [16] Gudmundsson V and Gerhardt R R 1991 *Phys. Rev. B* **43** 12 098
- [17] Zhu J-L, Li Z Q, Yu J Z, Ohno K and Kawazoe Y 1997 *Phys. Rev. B* **55** 15 819
- [18] Merkt U, Huser J and Wagner M 1991 *Phys. Rev. B* **43** 7320
- [19] Jacques J, De Groote S, Hornos J E M and Chaplik A V 1992 *Phys. Rev. B* **46** 12 773
- [20] Wagner M, Merkt U and Chaplik A V 1992 *Phys. Rev. B* **45** 1951
- [21] Zhu J-L, Cheng Y and Xiong J-J 1990 *Phys. Rev. B* **41** 10 792
- [22] Peeters F M and Schweigert V A 1996 *Phys. Rev. B* **53** 1468
- [23] Zhu J-L and Xu S 1994 *J. Phys.: Condens. Matter* **6** L299
- [24] Riva C, Schweigert V A and Peeters F M 1998 *Phys. Rev. B* **57** 15 392